Conformally invariant free-parafermionic quantum chains with multispin interactions

Francisco C. Alcaraz [*] and Lucas M. Ramos [†]
Instituto de Física de São Carlos, Universidade de São Paulo, Caixa Postal 369, 13560-970, São Carlos, SP, Brazil

(Received 16 February 2024; accepted 21 March 2024; published 16 April 2024)

We calculate the spectral properties of two related families of non-Hermitian free-particle quantum chains with N-multispin interactions ($N = 2, 3, \ldots$). The first family have a $Z(N)$ symmetry and are described by free parafermions. The second have a $U(1)$ symmetry and are generalizations of XX quantum chains described by free fermions. The eigenspectra of both free-particle families are formed by the combination of the same pseudo-energies. The models have a multicritical point with dynamical critical exponent $z = 1$. The finite-size behavior of their eigenspectra, as well as the entanglement properties of their ground-state wave function, indicate the models are conformally invariant. The models with open and periodic boundary conditions show quite distinct physics due to their non-Hermiticity. The models defined with open boundaries have a single conformal invariant phase, while the XX multispin models show multiple phases with distinct conformal central charges in the periodic case.

DOI: 10.1103/PhysRevE.109.044138

I. INTRODUCTION

Exactly integrable quantum chains with a free-particle eigenspectrum plays an important role in the understanding of many body physics. They are simple models and in general are solved by the standard Jordan-Wigner transformation [1,2]. Due to this transformation most of these models are mapped into an effective Hamiltonian formed by the addition of bilinear fermionic operators, whose solutions follows from a generalized Fourier transformation (Bogoliubov transformation). Recently a large class of free-particle quantum chains that are not bilinear after the Jordan-Wigner transformation were introduced. These are models defined in terms of $Z(N)$ parafermionic operators ($N = 2, 3, \ldots$), containing multispin interactions involving $(p+1)$-spins ($p = 1, 2, \ldots$). The exact solutions are known only when the quantum chains are defined in a lattice with an open boundary condition (OBC). In the case $p = 1$ and $N = 2$ they recover the standard free-fermionic quantum chain with two spin interactions. The simplest case, where $p = 2$ and $N = 2$, is the free fermionic Fendley three-spin multispin interacting model [3]. The cases where $p = 1$ and $N > 2$ are the free-parafermionic Baxter models [4–11]. The general cases where p and N are arbitrary were solved in [12,13]. This was done by extending the Fendley solution [3] for the fermionic case $N = 2$ and $p = 2$. The fermionic cases ($N = 2$) with general values of p are particular cases of free-fermion models defined in frustration graphs [14,15]. A more general related free-fermion model was also introduced recently [16].

Although the eigenenergies are exactly known for OBC the eigenfunctions are not known in a direct form. Interestingly the models show a phase diagram with a multicritical point with dynamical critical exponent $z = \frac{p+1}{N}$ [12,13], indicating that in general $z \neq 1$, and these models are not conformally invariant. Since most of the known critical quantum chains are conformally invariant, these exactly quantum chains provide an interesting laboratory to explore more general physical behaviors.

A natural question concerns the cases where $p + 1 = N$ and $z = 1$. Are the models conformally invariant in this case? Since conformal invariance imply, in the finite-size geometry, the existence of conformal towers in the eigenspectra, it is possible, from the exactly known eigenspectra, to verify this symmetry. It is interesting to mention that the ground-state energy of those non-Hermitian quantum chains ($N > 2$) is real and the eigenenergies of the excited states appear in complex conjugated pairs. Also these quantum chains have no chiral symmetry, but in some cases they have a parity-time (PT) reversal symmetry. This PT symmetry, however, is broken since the eigenenergies appear in complex conjugated pairs [17].

In Ref. [18] it was shown that for $N > p$ there exist a set of XX quantum chains with OBC that share the same quasi-energies that give the eigenenergies of the $Z(N)$ symmetric-free quantum chains. The Hamiltonian besides two-body interactions also contains $(p+1)$-multispin interactions. The equivalence happens up to overall degeneracies, mainly because the quasi-energies appear in distinct combinations in both models. These XX models have a $U(1)$ symmetry and are also non-Hermitian. Although sharing the eigenspectrum with a parafermionic model they are described by fermionic operators through the Jordan-Wigner transformation.

The spectral equivalence among the $Z(N)$ and XX Hamiltonians is valid for the OBC case. In the case of periodic boundary conditions (PBCs) where the exact solution for the exact eigenspectrum of the $Z(N)$ model is unknown for $N > 2$, the solution for the related XX model is simple due to its free fermionic formulation. In this paper we explore the equivalence of the $Z(N)$ and XX models to verify if indeed

[*] alcaraz@ifsc.usp.br
[†] lucas.morais@ifsc.usp.br

for the models where $N = p + 1$ ($z = 1$) the eigenspectrum is the one expected for quantum chains conformally invariant.

The paper is organized as follows. In Sec. II we present the free-particle models described in terms of fermionic and parafermionic operators. We present the models with $Z(N)$ symmetry and the related XX models with the larger $U(1)$ symmetry. In Sec. III we consider the solution of the models with OBC. The finite-size scaling of the eigenspectra of the models with OBC is given in Sec. IV. In Sec. V the eigenspectra of the periodic XX model are studied. In Sec. VI we present the entanglement properties of the XX models with multispin interactions and PBC. Finally in Sec. VII we draw our conclusions.

II. FREE-FERMIONIC AND FREE-PARAFERMIONIC QUANTUM CHAINS

Recently in [12,13] it was shown that a large family of quantum chains have a free-particle spectra. These are Hamiltonians written as the sum of M generators $\{h_i\}$,

$$H_M^{(N,p)}(\lambda_1, \ldots, \lambda_M) = -\sum_{i=1}^{M} \lambda_i h_i, \tag{1}$$

where $N = 2, 3, \ldots$, and $p = 1, 2, \ldots$ are integers, and λ_i are arbitrary coupling constants. The free-particle eigenspectra are a consequence of the $Z(N)$ exchange algebra, satisfied by the generators

$$\begin{aligned} &h_i h_{i+m} = \omega h_{i+m} h_i \quad \text{for} \quad 1 \leqslant m \leqslant p; \quad \omega = e^{i2\pi/N}, \\ &[h_i, h_j] = 0 \text{ for } |j - i| > p, \end{aligned} \tag{2}$$

with the closure relation

$$h_i^N = 1. \tag{3}$$

Any representation of $\{h_i\}$ $(i = 1, \ldots, M)$ will have a free-particle eigenspectrum. The eigenenergies, apart from an overall representation-dependent degeneracy (produced by zero modes), are given by

$$E_{s_1,\ldots,s_{\overline{M}}} = -\sum_{i=1}^{\overline{M}} \omega^{s_i} \varepsilon_i, \tag{4}$$

where

$$\overline{M} \equiv \text{int}\left(\frac{M+p}{p+1}\right) = \left\lfloor \frac{M+p}{p+1} \right\rfloor, \tag{5}$$

and $s_i = 0, 1, \ldots, N-1$ and ε_i $(i = 1, \ldots, \overline{M})$ are the quasienergies of the pseudoparticles forming the eigenspectra.

In Fig. 1 we show schematically some eigenenergies for the $Z(3)$ model [Figs. 1(a) and 1(b)] and for the $Z(5)$ model [Figs. 1(c) and 1(d)], in the case $\overline{M} = 3$. Figures 1(a) and 1(c) give a real eigenvalue and correspond in (4) to the ground-state energy of the chains. The 3^3 and 5^3 energies for the $Z(3)$ and $Z(5)$ models are obtained by considering all the three or five allowed positions in the circles of radius ϵ_1, ϵ_2, and ϵ_3, respecting a "circle exclusion principle" that allows *one and only one* excitation in each circle. This is the $Z(N)$ parafermionic generalization of the standard $Z(2)$ Fermi-exclusion principle. The pseudo-energies $\varepsilon_i = 1/z_i^{1/N}$

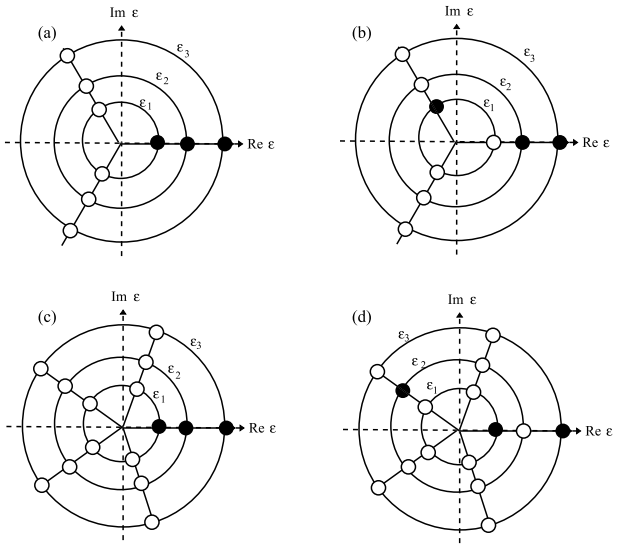

FIG. 1. Representation in the complex plane of the eigenenergies (4) with $\overline{M} = 3$, for the $Z(N)$ models with $N = 3$ (a), (b) and $N = 5$ (c), (d). The circles have the radius ε_i, and the possible values (open circles) are the intercepts with the $Z(N)$ circles. Each circle contributes with *one and only one* of the possible N intercepts (black circles).

are obtained from the roots z_i of a polynomial $P_{\overline{M}}(z)$, generated by the recurrence relation

$$P_j(z) = P_{j-1}(z) - z\lambda_j^N P_{j-(p+1)}(z), \; j = 1, 2, \ldots, \tag{6}$$

with the initial condition

$$P_j(z) = 1, \quad j \leqslant 0. \tag{7}$$

From (4), the representation of (2) with $N = 2$ will give us the Hamiltonian (1) with a free-fermion eigenspectrum, while for $N > 2$ we have the $Z(N)$ free-parafermionic ones.

An interesting general representation of (2) is given in terms of its independent words (word representation) (see Refs. [12,13]). The Hamiltonian is given by

$$\begin{aligned} H_M^{(N,p)} = &-\sum_{i=1}^{p} \lambda_i \left(\prod_{j=1}^{i-1} Z_j\right) X_i \\ &-\sum_{i=p+1}^{M} \lambda_i \left(\prod_{j=i-p}^{i-1} Z_j\right) X_i, \end{aligned} \tag{8}$$

where Z and X are the generalized $N \times N$ Pauli matrices satisfying

$$XZ = \omega ZX, \quad X^N = Z^N = 1, \quad Z^+ = Z^{N-1}. \tag{9}$$

The models contain $p + 1$ multispin interactions and, except for $N = 2$, are non-Hermitian. We stress that, for $N > 2$, the integrability is known only for OBC. For $N = 2$ and $p = 1$ we have the M-sites Ising-like model

$$H_M^{(2,1)} = \lambda_1 \sigma_1^x - \lambda_2 \sigma_1^z \sigma_2^x + \cdots + \lambda_M \sigma_{M-1}^z \sigma_M^x, \tag{10}$$

where σ^x, σ^z are the standard spin-$\frac{1}{2}$ Pauli matrices. Another representation for $N = 2$, $p = 1$, and M odd is the standard

quantum Ising chain with inhomogeneous couplings $\{\lambda_i\}$ and OBC

$$H_{\rm Ising} = -\sum_{i=1}^{L} \lambda_{2i-1}\sigma_i^x - \sum_{i=1}^{L-1} \lambda_{2i}\sigma_i^z\sigma_{i+1}^z, \tag{11}$$

with $L = (M+1)/2$ sites. We can show that the Hamiltonians (10) and (11) share the same eigenenergies and degeneracies.

The case where $N = 2$ and $p = 2$ in (8) is the three-spin interacting Fendley model:

$$H_M^{(2,2)} = -\lambda_1\sigma_1^x - \lambda_2\sigma_1^z\sigma_2^x - \lambda_3\sigma_1^z\sigma_2^z\sigma_3^x - \lambda_4\sigma_2^z\sigma_3^z\sigma_4^x - \cdots - \lambda_{M-1}\sigma_{M-3}^z\sigma_{M-2}^z\sigma_{M-1}^x - \lambda_M\sigma_{M-2}^z\sigma_{M-1}^z\sigma_M^x. \tag{12}$$

The phase diagram of this model, in the homogeneous case $\lambda_1 = \ldots, \lambda_M$ was studied in [3] and [19].

For $p = 1$ and arbitrary N the Hamiltonian (8) is given by (10) with the change $\sigma_i^x \to X_i$, $\sigma_i^z \to Z_i$ [satisfying (9)].

Another representation in the case $p = 1$, sharing the same eigenspectra is given by the known $Z(N)$ free-parafermionic Baxter model [4–6]

$$H_{\rm Baxter}^{(N)} = -\sum_{i=1}^{L} \lambda_{2i-1}X_i - \sum_{i=1}^{L-1} \lambda_{2i}Z_iZ_{i+1}^+, \tag{13}$$

with $L = (M+1)/2$ sites.

Another special model we are going to study in this paper is the $Z(3)$ version of the Fendley model, i.e., $p = 2$ and $N = 3$ in (8):

$$H_M^{(2,3)} = -\lambda_1X_1 - \lambda_2Z_1X_2 - \lambda_3Z_1Z_2X_3 - \lambda_4Z_2Z_3X_4 - \cdots - \lambda_{M-1}Z_{M-3}Z_{M-2}X_{M-1} - \lambda_MZ_{M-2}Z_{M-1}X_M. \tag{14}$$

It was shown for $N = 2$, $p = 1, 2$ in [3] and for general N, p in [12,13] that the isotropic point $\lambda_i = 1$ $(i = 1, \ldots, M)$ is a multicritical point with the energy gap vanishing as $\sim M^{-z}$, with the dynamical critical exponent value $z = (p+1)/N$. This means that in general $z \neq 1$ and the long-distance physics of the critical spin is not described by a conformal field theory (CFT). However, for the special set of models where $p + 1 = N$, the dynamical critical exponent $z = 1$, and the underlying field theory is relativistic and possibly conformal invariant. This is the case for $p = 1$ and $N = 2$, that we recover the standard critical Ising quantum chains [(11) with $\lambda_i = 1$]. However, for $N = p + 1 > 2$ the time-evolution operator (the Hamiltonian) is non-Hermitian.

In the following sections we are going to compute the finite-size spectrum of these Hamiltonians with $N = p + 1 > 2$ and verify the appearance of conformal towers as happens in the conformally invariant quantum chains.

III. GENERALIZED *XX* QUANTUM CHAINS WITH MULTISPIN INTERACTIONS

In [18,20] it was introduced a family of XX quantum chains with two- and N-multispin interactions, with a free-fermion eigenspectrum whose quasienergies are the same as the N-multispin interacting $Z(N)$ models discussed in the previous section. The Hamiltonian is given by

$$H_N^{XX} = \sum_{i=1}^{L-1} \sigma_i^+\sigma_{i+1}^- + \sum_{i=1}^{L-N+1} \lambda_i^N\sigma_i^- \left(\prod_{j=i+1}^{i+N-2} \sigma_j^z\right)\sigma_{i+N-1}^+, \tag{15}$$

where $\sigma^\pm = (\sigma^x \pm \sigma^y)/2$ are the standard raising/lowering spin-1/2 operators, $\{\lambda_i^N\}$ are the coupling constants, and the lattice size is $L = M + N - 1$.

It is interesting to observe that (15) under the parity symmetry (PT), where $i \to L - i + 1$, the Hamiltonian transforms as $H_N^{XX} \to (H_N^{XX})^\dagger$, and from [17], the Hamiltonian although non-Hermitian can produce a unitary evolution. The Hamiltonian (8) with $p = 1$ has a PT symmetry [21], but not for general values of p.

Differently from the $Z(N)$ models of last section the XX Hamiltonians have a $U(1)$ invariance, since $\sum_{j=1}^{L} \sigma_j^z$ is a good quantum number. In the simplest case where $N = 2$ the model recovers the dimerized version of the standard two-body XX model:

$$H_2^{XX}(\{\lambda_i\}) = \sum_{i=1}^{L-N+1} \sigma_i^+\sigma_{i+1}^- + \sum_{i=1}^{L-N+1} \lambda_i^2\sigma_i^-\sigma_{i+1}^+, \tag{16}$$

whose eigenspectrum is well known to be related with the quantum Ising chain [22].

The model (15), differently from (1) and (2), is bilinear in terms of fermionic operators $\{c_i\}$ obtained from the Jordan-Wigner transformation [1]

$$c_i = \sigma_i^- \prod_{j=1}^{i-1} \sigma_j^z, \quad c_i^\dagger = \sigma_i^+ \prod_{j=1}^{i-1} \sigma_j^z, \tag{17}$$

for $i = 1, \ldots, L$, that satisfy the anticommutation relations

$$\{c_i, c_j^\dagger\} = \delta_{i,j}, \quad \{c_i, c_j\} = \{c_i^\dagger, c_j^\dagger\} = 0. \tag{18}$$

Since $\sigma_j^z = 2c_j^\dagger c_j - 1$, the $U(1)$ symmetry is translated into the conservation of the total number of fermions $N_F = \sum_{i=1}^{L} c_i^\dagger c_i$, and the z magnetization of the XX multispin model is given by

$$m_z = \sum_{j=1}^{L} \sigma_j^z = 2N_F - L. \tag{19}$$

In terms of $\{c_i\}$ the Hamiltonian (15) has the bilinear form

$$H = -\sum_{i,j=1}^{L} c_i^\dagger \mathbb{A}_{i,j} c_j, \tag{20}$$

where

$$\mathbb{A}_{i,j} = \delta_{j,i+1} + \lambda_j^N \delta_{j,i+1-N} \tag{21}$$

are the elements of the matrix formed by the hopping coupling constants.

The matrix $\mathbb{A}$ for $N > 2$ is nonsymmetric but nevertheless can be diagonalized,

$$H = -\sum_{k=1}^{L} \Lambda_k \eta_k^\dagger \eta_k, \tag{22}$$

through the canonical transformation $\{c_i, c_i^\dagger\} \to \{\eta_k, \eta_k^\dagger\}$,

$$\eta_k = \sum_i^L \mathbb{L}_{i,k} c_i, \quad \eta_k^\dagger = \sum_i^L \mathbb{R}_{i,k} c_i^\dagger, \tag{23}$$

where in (22) Λ_k are the eigenvalues of $\mathbb{A}$ and $\mathbb{L}_{i,k}, \mathbb{R}_{i,k}$ are the components of the left and right eigenvectors with the normalization $\mathbb{R}\mathbb{L}^T = \mathbb{1}$, respectively.

From (22) the eigenenergies of H_N^{XX} have the free-fermion structure

$$H = -\sum_{k=1}^{M+N-1} s_k \Lambda_k, \quad s_k = 0, 1. \tag{24}$$

The quasienergies $\{\Lambda_k\}$ are obtained from the roots of $\det(\mathbb{A} - \Lambda_k \mathbb{1}) = 0$. Apart from the zero modes they are given by $\Lambda_k = 1/z_k^{1/N}$, where z_k are the roots ($P_M^{(N)}(z_k) = 0$) of the characteristic polynomial

$$P_M^{(N)}(z) \equiv \det(\mathbb{1} - z\mathbb{A}). \tag{25}$$

From the Laplace cofactor's rule for determinants, these polynomials satisfy the recurrence relations:

$$P_M^{(N)}(z) = P_{M-1}^{(N)}(z) - z\lambda_M^N P_{M-N}^{(N)}(z), \tag{26}$$

with the initial condition

$$P_M^{(N)}(z) = 1, \text{for } M \leqslant 0, \tag{27}$$

and $z_k = (1/\Lambda_k)^N$. Comparing (6) and (7) and (26) and (27) we see that the polynomials $P_M^{(N)}(z)$ are the same as those fixing the eigenspectra of the $Z(N)$ multispin chains with $N = p + 1$. Namely, the same roots $\{z_k\}$ that give the quasienergies $\epsilon_k = 1/z_k^{1/N}$ of the $Z(N)$ free-parafermionic multispin models also give the ones of the XX chains with N-multispin interactions,

$$\Lambda_{j,i} = e^{\frac{2\pi}{N} j} \epsilon_i, \tag{28}$$

where $i = 1, \ldots, \lfloor \frac{L}{N} \rfloor$ and $j = 0, 1, \ldots, N-1$. Since the dimension of H_N^{XX} is 2^L and the total number of nonzero quasienergies $\{\epsilon_i\}$ is L, we should have $N_z = L - N\lfloor \frac{L}{N} \rfloor$ zero modes, producing a 2^{N_z}-global degeneracy of the whole eigenspectra of the Hamiltonian

$$E_{\{s_{i,j}, r_{i,j}\}} = -\sum_{i=1}^{\lfloor \frac{L}{N} \rfloor} \left(\sum_{j=0}^{N-1} r_{i,j} \omega^{s_{i,j}} \right) \varepsilon_i, \tag{29}$$

where for each $i = 1, \ldots, \lfloor \frac{L}{N} \rfloor$, we have a possible $s_{i,j} = 0, 1, \ldots, N-1$ and $r_{i,j} = 0, 1$.

The schematic representations, similarly as shown in Fig. 1 for the $Z(3)$ model, are in circles of radius ϵ_i, but now in a given circle we have 2^N possible occupations of pseudoparticles. All the eigenenergies represented in Fig. 1 for the $Z(3)$ model are also presented in the three-multispin XX model, including the ground-state energy. The eigenlevels shown in Fig. 2 are present in the XX multispin model, but not in the corresponding $Z(3)$ $p = 2$ model with $\overline{M} = 2$, since they do not obey the circle exclusion constraint. The circle exclusion in the $Z(N)$ models is not a constraint for these $U(1)$ XX models.

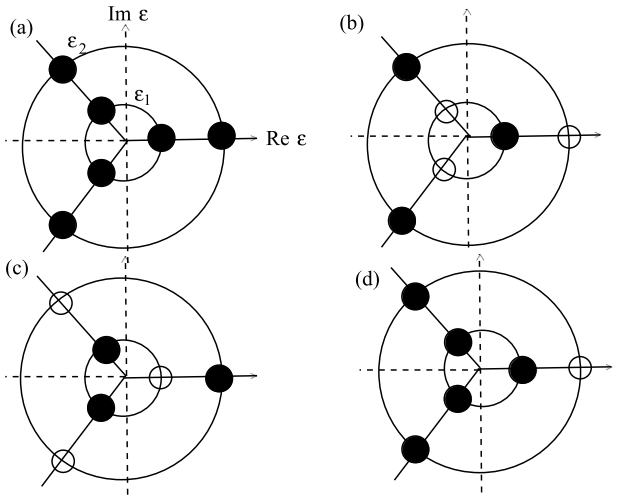

FIG. 2. Representation of configurations that are present in the $N =$ three-multispin XX quantum chains (29) but not present in the multispin $Z(3)$ quantum chain (4), in the case $\overline{M} = 2$. The circles have the radius ε_i, and the possible values (open circles) are the intercepts with the $Z(N)$ circles. Distinct from the configurations in Fig. 1, each circle may have multiple contributions (black circles), and do not satisfy the $Z(N)$ circle exclusion constraint.

IV. THE EIGENSPECTRA OF THE N-MULTISPIN INTERACTION MODELS WITH OPEN BOUNDARY CONDITIONS (OBC)

In this section we calculate the eigenenergies of the model with N-multispin interactions with $Z(N)$ and $U(1)$ symmetries presented in Secs. II and III, with OBC. We restrict ourselves to the isotropic couplings case where $\lambda_i = \lambda$ ($i = 1, \ldots, M$). In this case the roots $z_i(\lambda)$ of the polynomial (6) that fix the quasienergies obey $z_i(\lambda) = z_i(1)/\lambda^N$ and the quasienergies $\epsilon_i(\lambda) = \lambda\epsilon_i(1)$. This implies that the eigenspectra of the Hamiltonian satisfy

$$H_{\rm OBC}(\lambda) = \lambda H_{\rm OBC}(1). \tag{30}$$

This also follows directly from (1) in the case of the $Z(N)$ multispin models. In the case of the N-multispin XX model it is not direct, but in Sec. V we give a canonical transformation of the spin variables that also show (30) directly.

At their isotropic point the models are critical with a dynamical critical exponent $z = 1$. They are given by (8) with $p = N + 1$ in the $Z(N)$ case and by (15) in the XX case.

The multispin $Z(N)$ Hamiltonian with M sites have the energies

$$E_{\{s_1, \ldots, s_{\overline{M}}\}} = -\sum_{i=1}^{\overline{M}} \omega^{s_i} \epsilon_i, \quad s_i = 0, 1, \ldots, N-1, \tag{31}$$

while the XX model with $L = M + N - 1$ sites have the energies

$$E_{\{t_{i,j},r_{i,j}\}} = -\sum_{i=1}^{\overline{M}} \left(\sum_{j=0}^{N-1} r_{i,j} \omega^{t_{i,j}} \right) \epsilon_i, \tag{32}$$

with $r_{i,j} = 0, 1$, $t_{i,j} = 0, 1, \ldots, N-1$, and from (5) $\overline{M} = \lfloor \frac{L}{N} \rfloor$.

The pseudo-energies ϵ_i $(i = 1, \ldots, \overline{M})$ are the same for both models and can be evaluated from the roots z_i of the polynomial (26), since $\epsilon_i = 1/z_i^{1/N}$, or directly from the diagonalization of the hopping matrix $\mathbb{A}$ given by (21). In the critical region the low-lying quasiparticles $\{\epsilon_i\}$ give the relevant excitations, and we should expect that as $M \to \infty$ they should vanish. This means that in this limit, the large roots of the polynomial (26) should diverge.

The roots $\{z_i\}$ are all real, and the eigenenergies of (31) and (32) are in general complex, due to the non-Hermicity of the Hamiltonian (8) and (15).

For convenience we order the quasienergies $\epsilon_1 < \epsilon_2 < \cdots < \epsilon_{\overline{M}}$, while the eigenenergies of the Hamiltonian we order in increasing order of their real part:

$$\Re(E_0) \leqslant \Re(E_1) \leqslant \Re(E_2) \leqslant \cdots . \tag{33}$$

The lowest eigenenergy, that gives the ground-state energy, is real and is given by

$$E_0(M) = -\sum_{i=1}^{\overline{M}} \epsilon_i. \tag{34}$$

The ground-state energy can be derived using the results of [13] and is given by

$$e_\infty = \lim_{M\to\infty} \frac{E_0}{M} = -\frac{1}{N\pi} \int_0^\pi \frac{\sin x}{\sin^{\frac{1}{N}}\left(\frac{x}{N}\right) \sin^{\frac{N-1}{N}}\left(\frac{(N-1)x}{N}\right)}$$
$$= -\frac{N \sin\left(\frac{\pi}{N}\right)}{(N-1)\pi}, \tag{35}$$

with the values

$$-\frac{2}{\pi}, -\frac{3\sqrt{3}}{4\pi}, -\frac{2\sqrt{2}}{3\pi}, -\sqrt{\frac{5-\sqrt{5}}{8\pi}}, \tag{36}$$

for $N = 2$–5, respectively.

In order to verify the conformal invariance of the models at their critical points, we are going to explore the consequences of the underlying conformal symmetry in the finite-size eigenspectrum of the quantum chains with OBC.

The finite-size amplitudes of the excited states will give us the surface exponents of the model. To each surface exponent x_s of the infinite system [23] we should expect, at the critical point, a tower of eigenenergies

$$\Re(E_s(M, r)) = E_0(M) + \frac{\pi v_s (x_s + r)}{M} + o(M^{-1}), \tag{37}$$

where $r = 0, 1, 2, \ldots$.

Since the pseudo-energies $\{\epsilon_i = 1/z_i^{1/N}\}$ in (31) and (32) depend on the roots $\{z_i\}$ of the polynomials (6) or (26) it is convenient to observe their asymptotic finite-size dependences. In the cases where the model is critical we should expect that the large roots diverge with the order of the polynomial. In [20] was introduced a method that allows us to evaluate these large roots for huge lattice sizes ($\sim 10^9$) by using standard quadruple-precision numerical calculations. The coefficients of the polynomial have quite small and large numbers. The method works if we have a good initial guess for the roots. For the largest root, the Laguerre bound (see Corollary 6.2.4 in [24]) is the initial value. After the evaluation of the largest root we produce good initial guesses for the other roots by exploring the size dependence of the largest root. With this procedure we evaluate the largest 10–12 roots for polynomials up to the order $M = 10^9$. The method was also tested in the random formulation of free-fermion models ($N = 2$), with $p = 1$ [20] and more recently for $p = 2$ models [25].

The prediction (37) indicates the leading behavior for the roots of the polynomial $P_M^{(N)}(z)$ given in (26) and (27):

$$\frac{1}{z_i^{1/N}} = \epsilon_i = \pi \frac{A_i^{(N)}}{M} = \pi \frac{A^{(N)}}{M} \left(x_s^{(N)} + i - 1\right), \tag{38}$$

for $i = 1, 2, \ldots$. The amplitude $A^{(N)}$ is proportional to the sound velocity and $x_s^{(N)}$ is a surface exponent.

Our numerical solutions for polynomial roots with M up to 10^9 corroborate the conformal invariance prediction (38) for the roots. The stability of the numerical values induces us to determine the exact values for $N = 2, 3, 4$, and 6:

$$A^{(2)} = 2, \quad A^{(3)} = 2\sqrt{3}, \quad A^{(4)} = 4\sqrt{2}, A^{(6)} = 12, \tag{39}$$

and for the case $N = 5$ the approximate numerical value

$$A^{(5)} = 8.506283. \tag{40}$$

The surface exponent values depend on the particular sequence of lattice sizes [mod(M, N) fixed], used to obtain the bulk limit $M \to \infty$. The results we obtain for $N = 2$ and $N = 3$ are

$$x_s^{(2)} = 1, \ [\text{mod}(M, 2) = 0 \text{ or } 1],$$
$$x_s^{(3)} = 7/6 \ [\text{mod}(M, 3) = 0], \quad x_s^{(3)} = 1/6 \ [\text{mod}(M, 3) = 1],$$
$$x_s^{(3)} = 5/6 \ [\text{mod}(M, 3) = 2], \tag{41}$$

while for $N = 4$,

$$x_s^{(4)} = 5/4 \ [\text{mod}(M, 4) = 0], \quad x_s^{(4)} = 1/2 \ [\text{mod}(M, 4) = 1],$$
$$x_s^{(4)} = 3/4 \ [\text{mod}(M, 4) = 2], \quad x_s^{(4)} = 1 \ [\text{mod}(M, 4) = 3]. \tag{42}$$

In order to illustrate the numerical results we show in Table I the ratios $A_i^{(N)}/A^{(N)}$, a conformal tower of the model with $N = 2 - 5$, for $M = 10^9 - N - 1$ [mod$(M, N) = 0$].

The finite-size dependence of the mas gaps (37) of the $Z(N)$ and XX models with N-multispin interactions can be obtained directly from the relations (38)–(40).

Let us consider initially the $Z(N)$ free-parafermionic models. The ground-state energy (real) is obtained [see (34)] by considering all the roots in the branch $\omega^0 = 1$ [as in Fig. 3(a)]. A sequence of mass gaps with lower real part is obtained by changing a root ϵ_i $(i = 1, 2, \ldots)$ in the ground state [see Fig. 3(a)] to the $\omega^1 = e^{i2\pi/N}$ or $\omega^{N-1} = e^{-i2\pi/N}$

TABLE I. Examples of estimates for the ratios $A_i^{(N)}/A^{(N)}$ for some conformal towers of the models with $N = 2$–5. The ratios are the ones of the lattice sizes $M = 10^9 - N - 1$, where $\mathrm{mod}(M, N) = 0$.

i	$A^{(2)}(i)/A^{(2)}$	$A^{(3)}(i)/A^{(3)}$	$A^{(4)}(i)/A^{(4)}$	$A^{(5)}(i)/A^{(5)}$
1	1	1.1669439	1.24987070	1.333553
2	2	2.1666355	2.24998504	2.333366
3	3	3.1666632	3.24997209	3.333367
4	4	4.1666613	4.24995483	4.333357
5	5	5.1666589	5.24993348	5.333337
6	6	6.1666562	6.24990804	6.333328
12	12	12.1666314	12.24966964	12.332937

branches [see Figs. 3(b) and 3(c)]

$$\Re(G_i) = \Re(\epsilon_i - \omega\epsilon_i) = \left[1 - \cos\left(\frac{2\pi}{N}\right)\right]\epsilon_i \tag{43}$$

($i = 1, 2, \ldots$). The relations (39) and (40) give us the sound velocity, in (37), for the models

$$\begin{aligned} v_s^{(2)} &= 2A^{(2)} = 4, \\ v_s^{(3)} &= 3A^{(3)}/2 = 3\sqrt{3}, \quad v_s^{(4)} = 4\sqrt{2}, \\ v_s^{(5)} &= A^{(5)}[1 - \cos(2\pi/5)] \approx 0.69098300, \\ v_s^{(6)} &= A^{(6)}[1 - \cos(2\pi/6)] = 1/2, \end{aligned} \tag{44}$$

and the conformal towers

$$x_s^{(N)} + i - 1, \quad i = 1, 2, \ldots, \tag{45}$$

given in (41) and (42).

The conformal anomaly c is also predicted from the leading finite-size behavior of the ground-state energy $E_0(L)$. At a critical point, this should behave asymptotically as [26]

$$\frac{E_0}{L} = e_\infty + f_s L - \frac{\pi c v_s}{24L} + o(L^{-1}), \tag{46}$$

where e_∞ and f_s are, respectively, the bulk limits of the ground-state and surface energy per site, and v_s and c are the sound velocity and the conformal anomaly. The use of the above prediction is not simple because L is the effective

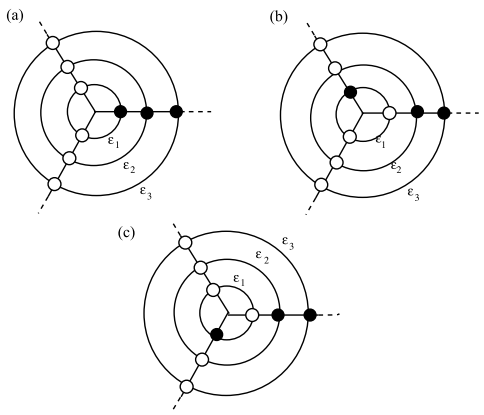

FIG. 3. Representation in the complex plane of the eigenenergies for the $Z(N)$ multispin model with $N = 3$. The configuration of the ground-state energy is (a), and (b) and (c) are the configurations that produce the lowest gaps (43).

number of sites of the space discretization of the underlying conformal field theory, and the relation with the number M in our models, except for the case $N = 2$, is not direct. To better explain this point we show below the expansions (46) up to order $o(M^{-2})$ for the cases $N = 2, 3$. For the case $N = 2$:

$$\begin{aligned} E_0 &= -\frac{2}{\pi}M + \left(1 - \frac{4}{\pi}\right) + \frac{\pi}{6M}, \quad \mathrm{mod}(M, 2) = 0, \\ E_0 &= -\frac{2}{\pi}M + \left(1 - \frac{4}{\pi}\right) - \frac{\pi}{12M}, \quad \mathrm{mod}(M, 2) = 1, \end{aligned} \tag{47}$$

while for $N = 3$:

$$\begin{aligned} E_0 &= -\frac{3\sqrt{3}}{4\pi}M - 0.46909 + \frac{1.9615}{M}, \quad \mathrm{mod}(M, 3) = 0, \\ E_0 &= -\frac{3\sqrt{3}}{4\pi}M - 0.46909 - \frac{0.5610}{M}, \quad \mathrm{mod}(M, 3) = 1, \\ E_0 &= -\frac{3\sqrt{3}}{4\pi}M - 0.46909 + \frac{1.6985}{M}, \quad \mathrm{mod}(M, 3) = 2. \end{aligned} \tag{48}$$

The expansion for $N = 2$ was calculated analytically and the one for $N = 3$ was obtained by a cubic fitting, considering $60 < M < 600$. The expansion in (47) with M odd recovers (46) if we identify the Ising quantum chain representation (11) with $M = 2L - 1$, $v_s = 2$ and $c = 1/2$. This is not the case for the expansion for $N = 2$ and M even, where the $O(1/M)$ term is positive instead of negative as in (46). The expansions for the $N = 3$ cases also give us terms that we cannot compare directly with (46). We leave the conformal anomaly calculations for the next section where we consider the periodic lattices.

We have also, in the $Z(N)$ models, the excited states formed by replacing ℓ ($\ell = 2, 3, \ldots$) quasienergies in the branch ω^0 by quasienergies in the branches ω^1 or ω^{N-1} (see Fig. 4). From (38) and (45) the mass gaps associated with these states give us the conformal dimensions

$$\ell x_s^{(N)} + j, \tag{49}$$

with $\ell, j \in \mathbb{Z}$ and $\ell \geqslant 1$ and $j \geqslant \ell(\ell + 1)/2$.

For $N > 3$ we can produce several other conformal dimensions since we can consider the eigenstates where the particles are in larger number of branches ω^n ($n = 0, \ldots, N - 1$).

For the case of the XX models with N-multispin interactions, we have the same quasienergies ϵ_i, considered in the $Z(N)$-parafermionic models, but their possible combinations are not restricted to the $Z(N)$ circle exclusion. This

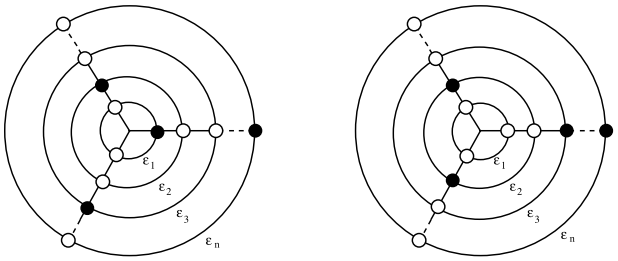

FIG. 4. Representation in the complex plane of the energies of some excited states for the $N = 3$ XX multispin model.

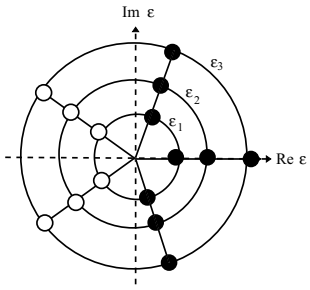

FIG. 5. Representation in the complex plane of the ground-state eigenenergy of the $N = 5$ multispin XX model.

implies that a given quasienergy ϵ_i can appear up to N times $(\omega^n\epsilon_i, n = 0, \ldots, N)$ in a given eigenenergy of the Hamiltonian. The model has now a $U(1)$ symmetry, and we can separate the associated eigenvector space according to its magnetization, or equivalently, to the number N_F of fermionic quasienergies. The magnetization is given by (19). For $N \leqslant 4$ the ground state is formed by taking all the $\overline{M} = \lfloor \frac{L}{N} \rfloor$ roots a single time in the branch $\omega^0 = 1$. It belongs to the sector where $m_z^{(0)} = 2\overline{M} - L$. This energy coincides with the ground-state energy of the corresponding $Z(N)$ parafermionic quantum chain. Actually all the eigenenergies we consider previously in the $Z(N)$ model are also present in the sector with magnetization $m_z^{(0)}$, giving us the same sound velocity and conformal dimensions given in (41)–(45). The absence of the $Z(N)$ circle exclusion gives additional conformal dimensions, inside the $m_z^{(0)}$ sector. They are formed by neglecting an arbitrary number of roots forming the ground state (branch ω^0) and inserting them in the other branches, keeping the number of fermions N_F fixed (some examples of excitations are shown in Fig. 4).

The conformal dimensions coming from the eigensectors with other magnetizations are obtained by neglecting and inserting distinct number of particles in the ground-state pseudoparticles configuration. It is simple to verify that some of the produced gap will give the same conformal dimensions (44)–(49), but with a distinct sound velocity that depends on the particular magnetization sector. This means that distinct from the $Z(N)$ parafermionic model, the XX multispin model in the bulk limit, is a combination of distinct theories with unequal sound velocities.

For $N > 4$ the ground-state energy of the related $Z(N)$ parafermionic quantum chain is in the sector $m_z^{(0)}$, but in the XX model it is an excited state. The energy with lowest real part in the XX model is obtained by adding all the roots in the branches $\omega^{\pm\ell}$ $(\ell = 0, 1, \ldots, \lfloor \frac{N-1}{2} \rfloor)$ (see Fig. 5) and gives

$$E_0 = -\left[1 + 2\sum_{\ell=1}^{\lfloor \frac{N-1}{4} \rfloor} \cos\left(\frac{2\pi}{N}\ell\right)\right] \sum_{i=1}^{\overline{M}} \epsilon_i. \tag{50}$$

V. THE N-MULTISPIN XX MODELS WITH PERIODIC BOUNDARY CONDITIONS (PBC)

The eigenspectral equivalence among the $Z(N)$ multispin models and the XX multispin quantum chains holds only in the case of OBC. Previous numerical studies [11] of the $Z(3)$ parafermionic Baxter model ($p = 1, N = 3$ in (8)) show us that the quantum chain with PBC have quite distinct properties from the chain with OBC. The energy per site of the ground-state energy of the different boundary conditions are distinct. We should expect a similar effect for the more general $Z(N)$ parafermionic quantum chains with multispin interactions (8).

In this section we are going to study the N-multispin XX models with isotropic couplings and PBC. The Hamiltonian has $L = M + N - 1$ sites and is given by

$$H_{\rm PBC}(\lambda) = H_{\rm OBC}(\lambda) + H_s^{(L)} + H_s^{(R)}, \tag{51}$$

where

$$H_{\rm OBC}(\lambda) = \sum_{i=1}^{L-1} \sigma_i^+\sigma_{i+1}^- + \lambda^N \sum_{i=1}^{L-N+1} \sigma_i^- \left(\prod_{j=i+1}^{i+N-2} \sigma_j^z\right) \sigma_{i+N-1}^+ \tag{52}$$

is the XX Hamiltonian with OBC and

$$H_s^{(L)} = \sigma_L^+\sigma_1^-, \tag{53}$$

$$H_s^{(R)} = \lambda^N \sum_{\ell=1}^{N-1} \sigma_{L+\ell-N+1}^- \times \left(\prod_{k=L+2+\ell-N}^{L} \sigma_k^z\right) \left(\prod_{t=1}^{\ell-1} \sigma_t^z\right) \sigma_\ell^+ \tag{54}$$

are the left and right surface terms.

It is interesting to consider the site-dependent canonical transformation,

$$\sigma_i^\pm \to (\lambda)^{\mp(i-1)}\sigma_i^\pm; \quad \sigma_i^z \to \sigma_i^z \quad (i = 1, \ldots, L), \tag{55}$$

that transforms the Hamiltonian (51) into

$$H_{\rm PBC}(\lambda) = \lambda H_{\rm OBC}(1) + \frac{1}{\lambda^{L-1}} H_s^{(L)} + \lambda^{L+1} H_s^{(R)}(1). \tag{56}$$

This result tell us that the spectral symmetry (30) holds only in the OBC case, and for $\lambda \neq 1$ we may expect distinct behavior for the PBC. This happens even in the bulk limit since the surface terms gave contributions that are exponentially large with the system's size.

The $U(1)$ symmetry of the model allows us to split the associated vector space of the Hamiltonian (51) into sectors

labeled by the z magnetization m_z. In each sector, where the number of fermion is $N_F = (m_z + L)/2$, we can perform the Jordan-Wigner transformation given in Sec. III, and the Hamiltonian (51) takes the form

$$H_{\rm OBC}(\lambda) = -\left(\sum_{i=1}^{L-1} c_i^\dagger c_{i+1} + \lambda^N \sum_{i=1}^{N} c_{i+N-1}^\dagger c_i\right), \tag{57}$$

$$H_s^{(L)} = -(-)^{L+N_F+1} c_L^\dagger c_1,$$

$$H_s^{(r)} = -(-)^{L+N_F+1} \sum_{\ell=1}^{N-1} c_\ell^\dagger c_{M+\ell}, \tag{58}$$

so that

$$H_{\rm PBC}(\lambda) = -\left(\sum_{i=1}^{L} c_i^\dagger c_{i+1}, +\lambda^N \sum_{i=1}^{L} c_{i+N-i}^\dagger c_i\right), \tag{59}$$

with the boundary condition

$$c_{L+\ell} = (-)^{L+N_F+1} c_\ell \quad (\ell = 1, 2, \cdots). \tag{60}$$

The fermionic model is periodic or antiperiodic depending if $L + N_F + 1$ is even or odd, respectively.

In order to diagonalize (59) we perform the Fourier transformation $\{c_i\} \to \{\eta_k\}$, where

$$\eta_k = \frac{1}{\sqrt{L}} \sum_{j=1}^{L} e^{ikj} c_j, \quad c_j = \frac{1}{\sqrt{L}} \sum_{\{k\}} e^{-ikj} \eta_k. \tag{61}$$

It follows from the algebraic relations of $\{c_j\}$ (18) that $\{\eta_j\}$ are also fermionic operators:

$$\{\eta_k, \eta_{k'}^\dagger\} = \delta_{k,k'}, \quad \{\eta_k, \eta_{k'}\} = 0. \tag{62}$$

Inserting (61) in (60) we obtain the sets

$$k_j = \begin{cases} \frac{2\pi j}{L}, & \text{if } L + N_F + 1 \text{ even} \\ \frac{2\pi (j+\frac{1}{2})}{L}, & \text{if } L + N_F + 1 \text{ odd} \end{cases}, \tag{63}$$

and $\{k_j\}$ are chosen inside one of the Brillouin zones, e.g., $-\pi < k_j \leqslant \pi$.

The Hamiltonian (56) in terms of $\{\eta_k\}$ is diagonal

$$H = \sum_{\{k_j\}} \epsilon(k_j) \eta_{k_j}^\dagger \eta_{k_j}, \tag{64}$$

where

$$\epsilon(k_j) = -\left(e^{-ik_j} + \lambda^N e^{i(N-1)k_j}\right), \tag{65}$$

and the momentum of a given state is $P = \sum_{\{k_j\}} \eta_{k_j}^\dagger \eta_{k_j}$.

As in the OBC we order the eigenvalues in increasing order of their real part. The effective dispersion relation is

$$\Lambda(k) = \Re[\epsilon(k)] = -\{\cos k + \lambda^N \cos[(N-1)k]\}. \tag{66}$$

This is also the dispersion relation of an extended Hermitian XX model, considered in [27]. The momentum and the real part of the eigenenergies for a given set of quasimomenta $\{k_j\}$ are given by

$$P = \sum_{\{k_j\}} k_j, \tag{67}$$

$$\Re(E(\{k_j\}) = \sum_{\{k_j\}} \Lambda(k_j). \tag{68}$$

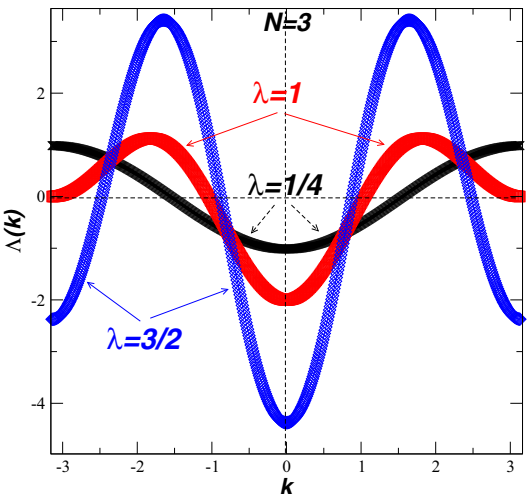

FIG. 6. Dispersion relation $\Lambda(k)$, given in (66), for the multispin XX quantum chain with $N = 3$ and some values of λ. The Fermi points are the ones where $\Lambda(k_F) = 0$.

The ground-state energy is formed by the combination of the quasienergies with negative values of $\Lambda(k)$,

$$\Re(E_0) = \sum_{k \in \{\Lambda(k) < 0\}} \Lambda(k). \tag{69}$$

We see directly from (66) that in the simplest case $N = 2$, $\Lambda(\lambda) = \frac{\lambda^2+1}{2}\Lambda(1)$, and from (64) the symmetry (30) that happens in the OBC is not present in the case of PBC if $\lambda \neq 1$. This means that for $\lambda \neq 1$ the ground-state energy per site has an anomalous behavior, being distinct for different boundary conditions.

Let us consider separately the quantum chains with distinct values of N.

1. $N = 3$. In Fig. 6 we show the dispersion relations $\Lambda(k)$ for the cases $\lambda = 2$, $\lambda = 1$ and $\lambda = 1/2$. The Fermi points ($\Lambda(k_F) = 0$) are given by

$$k_F = \arccos\left(\frac{-1 \pm \sqrt{1 + 8\lambda^6}}{4\lambda^3}\right). \tag{70}$$

We can show that for $\lambda \leqslant 1$ (see Fig. 6) we have two Fermi points $(k_F^{(1)}, k_F^{(2)})$ while for $\lambda > 1$ we have four of them $(k_F^{(1)}, \ldots, k_F^{(4)})$. The ground-state energy is real and obtained from the addition of the quasienergies with $\Lambda(k_j) < 0$,

$$E_0 = -\sum_{\ell=1}^{N_{FP}/2} \sum_{k_F^{(2\ell-1)} \leqslant k_j \leqslant k_F^{(2\ell)}} [\cos k_j + \lambda^3 \cos(2k_j)], \tag{71}$$

where the number of Fermi points $N_{FP} = 2$ if $\lambda \leqslant 1$ and 4 if $\lambda > 1$. Since $\Delta k = k_{j+1} - k_j = \frac{2\pi}{L}$ we have in the bulk limit

$$e_\infty(\lambda) = \lim_{L\to\infty} \frac{E_0}{L}$$

$$= -\frac{1}{2\pi} \sum_{\ell=1}^{N_{FP}/2} \int_{-k_F^{(2\ell-1)}}^{k_F^{(2\ell)}} [\cos k + \lambda^3 \cos(2k)]\, dk$$

$$= -\frac{1}{2\pi} \sum_{\ell=1}^{N_{FP}} (-)^\ell \left[\sin k_F^{(\ell)} + \lambda^3 \sin\left(2k_F^{(\ell)}\right)\right]. \tag{72}$$

At $\lambda = 1$, $k_F^{(1)} = -\frac{\pi}{3}$, $k_F^{(2)} = \frac{\pi}{3}$ and

$$e_\infty = -\frac{1}{2\pi}\int_{-\frac{\pi}{3}}^{\frac{\pi}{3}} [\cos k + \lambda^3 \cos(2k)]\, dk = -\frac{3\sqrt{3}}{4\pi}, \quad (73)$$

which coincides with the conjectured value obtained in the OBC case. For $\lambda \neq 1$ the values obtained from (71) and (72) are distinct from the prediction $-\lambda\frac{3\sqrt{3}}{4\pi}$ of the OBC [see (30)], similarly as happens with the $Z(3)$ free-parafermionic Baxter model [11].

In order to verify the conformal invariance of the model, let us compute the conformal towers that should appear in the leading $L \to \infty$ finite-size behavior of the eigenenergies of the Hamiltonian.

Conformally invariant critical systems, with PBC, should have a ground-state energy $E_0^{(0)}(L)$, with the asymptotic finite-size behavior [26,28]

$$\frac{E_0^{(0)}(L)}{L} = e_\infty - \frac{\pi v_s c}{6L^2} + o(L^{-2}), \quad (74)$$

where e_∞ is the ground-state energy per site in the bulk limit, c is the conformal anomaly, and v_s is the sound velocity, obtained from the energy-momentum dispersion relation. Moreover, for each operator [23] $\mathcal{O}_\alpha$ with dimension x_α in the operator algebra of the underlying conformal field theory, there exists an infinite tower of eigenstates in the quantum chain, that for L sites and PBC should behave as

$$E_{j,j'}^{\alpha}(L) = E_0^{(0)} + \frac{2\pi v_s}{L}(x_\alpha + j + j') + o(L^{-1}). \quad (75)$$

Let us consider initially the case $\lambda = 1$. We take the finite-size sequences of even lattice sizes: $L = 2\ell$, $\ell \in \mathbb{Z}$. The Fermi momentum are $k_F = \pm\frac{\pi}{3}$, and the ground-state energy is obtained by taking the symmetric distribution of $N_F = \frac{L}{3}$ fermions (even) and quasimomenta $k_j = \frac{2\pi}{L}(j + \frac{1}{2})$, $j = -\frac{L}{6}, \ldots, \frac{L}{6} - 1$. This will give us from (67) a zero momentum state ($P = 0$), and the sums in (68) give us the exact result:

$$\frac{E_0^{(0)}}{L} = -\frac{\sqrt{3}}{4\sin(\pi/L)}\left(2 + \frac{1}{\cos(\pi/L)}\right). \quad (76)$$

The expansion for $L \to \infty$ gives

$$\frac{E_0^{(0)}}{L} = -\frac{3\sqrt{3}}{4\pi} - \frac{\sqrt{3}\pi}{4L^2} - \frac{7\sqrt{3\pi^3}}{80L^4} + O(L^{-6}). \quad (77)$$

Comparing this result with the prediction (74) we obtain $v_s c = \frac{3\sqrt{3}}{2}$. On the other hand, the sound velocity can be obtained from the energy-momentum dispersion at the Fermi momentum

$$v_s = \left.\frac{\partial E_0^{(0)}}{\partial k}\right|_{k=k_F} = \left.\frac{d\Lambda(k)}{dk}\right|_{k=k_F} = \sin k_F + 2\lambda^3 \sin(2k_F), \quad (78)$$

which for $\lambda = 1$ gives $v_s = 3\sqrt{3}/2$.

We see from (77) and (36) that the ground-state energy per site is the same for the PBC and OBC at $\lambda = 1$, differently from the case of the $Z(3)$ $p = 1$ free-parafermionic Baxter chain, where they depend on the particular boundary condition [11]. However, even for $\lambda = 1$ the sound velocity $v_s = 3\sqrt{3}/2$ for the PBC is half of the value obtained for the OBC (44). This anomalous behavior, even at $\lambda = 1$, for the distinct boundaries is a consequence of the non-Hermiticity of the Hamiltonian.

The eigensector containing the ground state have $N_F = \frac{L}{3}$ fermions and magnetization $m_z = -L/3$. We label the $U(1)$ symmetry charges relative to the ground state as

$$Q = N_F - \frac{L}{3}, \quad (79)$$

so that the ground state has zero momentum and charge $Q = 0$. In the ground-state sector ($Q = 0$) we can create a state with momentum $P = \frac{2\pi}{L}$ (or $P = -\frac{2\pi}{L}$) by changing in the ground-state energy the quasimomentum $k_{\ell-1}$ (or $-k_\ell$) to the one with k_ℓ (or $k_{\ell+1}$), producing the mass gap

$$\begin{aligned}\Re(G(\pm p)) &= E_0^{(0)} - \Lambda(k_{\ell-1}) + \Lambda(k_\ell) \\ &= E_0^{(0)} - \Lambda(-k_\ell) + \Lambda(-k_{\ell+1}),\end{aligned} \quad (80)$$

whose L-large expansion gives

$$\Re[G(\pm p)] = \frac{2\pi v_s}{L} - \frac{3\sqrt{3}\pi^3}{2L^2} + O(L^{-4}). \quad (81)$$

Excited states with other momentum values, in the ground-state sector, are obtained by changing quasiparticles from below to above the Fermi momentum.

The lowest eigenenergy with $N_F = \frac{L}{3} + 1$ ($N_F = \frac{L}{3} - 1$) belonging to the sector $Q = 1$ ($Q = -1$) is obtained by taking in (67) $k_j = \frac{2\pi}{L}$, $j = -\frac{L}{6}, \ldots, \frac{L}{6} - 1, \frac{L}{6}$ ($j = -\frac{L}{6}, \ldots, \frac{L}{6} - 1$) and is given by

$$\frac{E_0^{(\pm 1)}}{L} = \frac{\sqrt{3}}{4L}\left[\tan\left(\frac{\pi}{L}\right) - 3/\tan\left(\frac{\pi}{L}\right)\right], \quad (82)$$

with the large-L dependence

$$\frac{E_0^{(\pm 1)}}{L} = -\frac{3\sqrt{3}}{4\pi} + \frac{\sqrt{3}\pi}{2L^2} + \frac{\sqrt{3}\pi^3}{10L^4} + O(L^{-6}), \quad (83)$$

giving us the gap

$$E_0^{(\pm 1)} - E_0^{(0)} = \frac{3\sqrt{3}\pi}{4L} + O(L^{-2}) = \frac{2\pi v_s}{L}\left(\frac{1}{4}\right) + O(L^{-2}).$$

The prediction (75) indicates the existence of a conformal operator with dimension $x = \frac{1}{4}$. The descendants of the operator will be related to the eigenenergies obtained by exciting the quasienergies that produce the lowest energy $E_0^{(\pm 1)}$. The lowest eigenenergies with $U(1)$ charge Q (or $-Q$) will have a zero momenta and are obtained by inserting (neglecting) symmetrically the quasiparticles forming the lowest energy configuration $E_0^{(0)}$ or $E_0^{(1)}$, depending if Q is even or odd. A simple calculation give us the mass gap

$$E_0^{(Q)} - E_0^{(0)} = \frac{2\pi v_s}{L}\frac{Q^2}{4} + O(L^{-2}), \quad (84)$$

and from (75) the related conformal dimensions are $Q^2/4$.

For a given sector Q, with a certain distribution $\{k_j\}$, the excitation where we take β quasienergies near the Fermi momentum from the positive (negative) branch and insert them

in the negative (positive) branch will give a set of mass gaps

$$\Re\big(E_0^{(Q,\beta)}\big) - E_0^{(0)} = \frac{2\pi}{L} v_s \left(\frac{Q^2}{4} + \beta^2 \right), \tag{85}$$

giving us the conformal dimension $Q^2/4 + \beta^2$. The descendants of these dimensions are obtained by exciting the particles in the positive and negative branches.

These results imply that the model is described by a Gaussian conformal field theory with wave number Q and vorticity β [29,30], and dimensions given by

$$x_{Q,\beta} = \frac{2\pi}{L} v_s \left(Q^2 x_p + \frac{\beta^2}{4x_p} \right), \tag{86}$$

where $x_p = 1/4$ and $Q, \beta = 0, \pm 1, \pm 2, \ldots$. This is precisely the same operator content of the standard $N = 2$ XX model ($\lambda = 1$) [31,32]. The only differences are the nonuniversal quantities e_∞, v_s and the z-magnetization associated with the $Q = 0$ sector, which is zero in the standard XX model and $L/3$ in the model with $N = 3$ ($\lambda = 1$).

For $\lambda < 1$ we obtain a similar operator content as is the case $\lambda = 1$, but with a sound velocity $v_s(\lambda)$ that depends on the Fermi momentum $\Lambda(k_F) = 0$, and given by (78). For example, for

$$\lambda^3 = \frac{\sqrt{5}-1}{1+\sqrt{5}} \approx 0.618034, \quad k_F = \frac{\pi}{5}, \tag{87}$$

the ground state belongs to the sector of magnetization $m_z = m_z^{(0)} = -3L/5$, with the leading finite-size behavior

$$\frac{E_0}{L} = e_\infty - \frac{\pi v_s}{6L^2} + O(L^{-4}), \tag{88}$$

where

$$e_\infty = -\frac{2\sqrt{5+\sqrt{5}} + \lambda^3 \sqrt{5-\sqrt{5}}}{4\sqrt{2}\pi},$$
$$v_s = \frac{\sqrt{5+\sqrt{5}} + 2\lambda^3 \sqrt{5-\sqrt{5}}}{4\sqrt{2}}. \tag{89}$$

The first excited state in the sector of magnetization $m_z = m_z^{(0)} \pm 1$, similarly as in (80) and (81), gives the energy gap

$$E^{(\pm 1)} - E_0 = \frac{2\pi v_s}{L} \frac{1}{4}. \tag{90}$$

The results (88) and (90) indicate we have for $\lambda < 1$ the same conformal towers that appeared in the $\lambda = 1$ case, only differing in the sound velocity $v_s(\lambda)$.

For $\lambda > 1$ we have now four Fermi points (see Fig. 6). Our results indicate that we have a composition of two central charge $c = 1$ theories. The sound velocities $v_s^{(1)}$ and $v_s^{(2)}$ in the branches $k_F^{(1)}$ and $k_F^{(4)}$ are distinct from the ones $v_s^{(2)}$ in $k_F^{(2)}$ and $k_F^{(3)}$. The ground-state energy has the leading finite-size behavior

$$\frac{E_0}{L} = e_\infty - \frac{\pi}{6L^2} \big(v_s^{(1)} + v_s^{(2)} \big) + O(L^{-4}). \tag{91}$$

The excitations that will give the dimensions x_p will give the same value $x_p = \frac{1}{4}$ in all branches. For example, for $\lambda = [\sin(3\pi/14)/\sin(\pi/14)]^{1/3}$, $k_F^{(2)} = -k_F^{(2)} = -2\pi/7$, and $k_F^{(1)} = -k_F^{(4)} \approx -0.7961934\pi$. The contribution to the ground-state energy for the branch $\frac{2\pi}{7} < k < \frac{2\pi}{7}$ has the leading behavior

$$\frac{E_0^{(1)}}{L} = \cos\left(\frac{\pi}{14}\right) \frac{\lambda^3 - 2 + 4\cos(\frac{\pi}{7})}{2\pi} - \frac{\pi v_s^{(1)}}{6L^2} + O(L^{-4}),$$

with

$$v_s^{(1)} = \cos\left(\frac{3\pi}{14}\right) + 2\lambda^3 \cos\left(\frac{\pi}{14}\right) \approx 4.74437,$$

while the contribution from $-\pi \leqslant k \leqslant k_F^{(1)}$ and $\pi - k_F^{(4)} \leqslant k < \pi$ gives

$$\frac{E_0^{(2)}}{L} \approx -0.683626 - \frac{\pi v_s^{(2)}}{6L^2} + O(L^{-4}),$$

with

$$v_s^{(2)} \approx 6.24521.$$

The excitations that contribute to the dimension x_p give $2\pi v_s^{(i)}/4$ ($i = 1, 2$), implying $x_p = 1/4$.

These results imply that for $\lambda > 1$ we have a mixture of two central charge $c = 1$ theories with distinct sound velocities, giving an effective theory with central charge $c = 2$. Consequently we have at $\lambda = \lambda_c = 1$ a phase transition from an effective theory with $c = 1$ ($\lambda \leqslant 1$) to another one with $c = 2$ ($\lambda > 1$).

2. $N = 4$. In Fig. 7 we show the dispersion relation $\Lambda(\lambda)$ for the cases $\lambda = 0.25$, 1. and 1.25. From (66) it follows that for $\lambda < \lambda_c = \frac{1}{3^{1/4}} \approx 0.7598$ there exist only two Fermi points $k_F = \pm\frac{\pi}{2}$ in the Brillouin zone $-\pi \leqslant k < \pi$. The ground state belongs to the sector with $m_z = L/2$ and has the leading finite-size behavior:

$$\frac{E_0}{L} = e_\infty - \frac{\pi v_s}{6L^2} + O(L^{-4}),$$
$$e_\infty = \frac{\lambda^4 - 3}{3\pi},$$
$$v_s = 3\lambda^4 - 1. \tag{92}$$

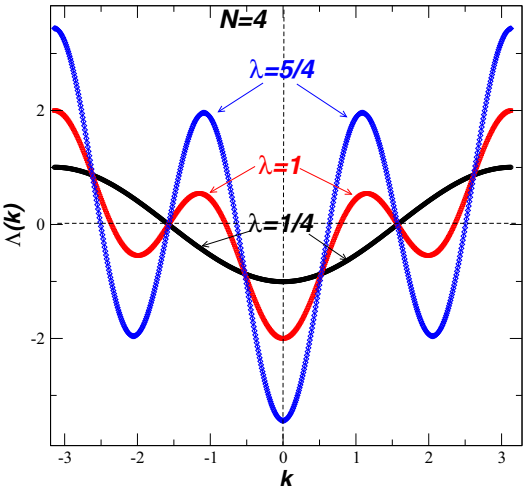

FIG. 7. Dispersion relation $\Lambda(k)$, given in (66), for the multispin XX quantum chain with $N = 4$, and some values of λ. The Fermi points are the ones where $\Lambda(k_F) = 0$.

The first excited state in the sector with magnetization $m_z = L/2 \pm 1$ gives the dimension $x_p = 1/4$, like in the former cases $N = 2$ and 3.

For $\lambda > \lambda_c$ appear four new Fermi points, and an analysis similar as in the case $N = 3$ shows us that we have the finite-size leading behavior for the ground-state energy:

$$\frac{E_0}{L} = e_\infty - \frac{\pi}{6L^2}\left(\sum_{i=1}^{6} v_s^{(i)}\right) + O(L^{-2}), \tag{93}$$

where

$$v_s^{(i)} = \left|\sin k_F^{(i)} - 3\lambda^4 \sin\left(3k_F^{(i)}\right)\right|, \tag{94}$$

and $k_F^{(i)}$ $(i = 1, \ldots, 4)$ are the Fermi momenta $(\Lambda(k_F^{(i)}) = 0)$.

We then have a quantum chain ruled by an effective $c = 3$ central charge theory, formed by the composition of three central charge $c = 1$ theories, all of them with the polarization operator with dimension $x_p = 1/4$. Actually these ground states are indeed excited states of the standard XX quantum chains, and the appearance of central charges proportional to the number of Fermi points (disjoint sectors of quasimomenta) was observed in [33], and also more recently in [34].

At $\lambda = 1$ the Fermi points are $-3\pi/4, -\pi/2, \pi/2, 3\pi/4$ and the value of $e_\infty = -\frac{2(1+2\sqrt{2})}{3\pi}$. This is distinct from the value $-\frac{2\sqrt{2}}{3\pi}$ given in (36) for the OBC. We see that the anomalous behavior verified numerically for the $p = 1$ $Z(3)$ free-parafermionic Baxter model [11] is observed analytically (even at $\lambda = 1$) for the $N = 4$-multispin XX model.

3. $N > 4$. We conjecture that for small values of $\lambda < \lambda_c^{(1)}$ we have always a $c = 1$ conformal spectrum and for large values $\lambda > \lambda_c^{(2)}$ the spectra if given by a mixture of $(N-2)$ $c = 1$ theories, giving us conformal towers of effective $c = N - 1$ conformal theories. The dimension that generates all the conformal dimensions (compactification ratio in the Coulomb gas language, or Luttinger parameter in spin liquid language) is always $x_p = 1/4$, as in the standard XX quantum chain. Actually, as we shall see in the next section, for the cases of the odd values of $N > 3$, there exist intermediate phases with smaller central charges [see (104) and (105)]. Again, we verified that the energy per site e_∞, even at $\lambda = 1$ is distinct for the PBC and OBC cases.

VI. THE ENTANGLEMENT ENTROPIES OF THE XX MULTISPIN INTERACTION QUANTUM CHAINS

A direct test of the conformal invariance of a given critical quantum chain is the evaluation of the entanglement entropy obtained from the pure state density matrix

$$\rho = |\Phi_L\rangle\langle\Phi_R|, \tag{95}$$

where $|\Phi_L\rangle$ and $\langle\Phi_R|$ are the left and right ground-state wave functions of the Hamiltonian. We split the chain of L sites in two disjoint sublattices A and B containing ℓ and $L - \ell$ contiguous sites, respectively. The reduced density matrices of the subsystems A and B are obtained from the partial trace of the complementary subsystem, i.e., $\rho_A = \mathrm{Tr}_B\rho$ and $\rho_B = \mathrm{Tr}_A\rho$. The α-Rényi entanglement entropy $(\alpha = 1, 2, \ldots)$ of subsystem A is defined as

$$S_\alpha(\ell, L) = \frac{1}{1-\alpha}\ln[\mathrm{Tr}\,(\rho_A)^\alpha]. \tag{96}$$

The limit $\alpha \to 1$ gives the von Neumann entanglement entropy

$$S_1(\ell, L) = -\mathrm{Tr}\,(\rho_A \ln \rho_A). \tag{97}$$

The conformal invariant quantum chains, i.e., the ones ruled by an underlying conformal field theory, have a leading behavior as $L \to \infty$ ($\frac{\ell}{L}$ fixed) for the α-Rényi entropy [35–38]

$$S_\alpha(L, \ell) = \frac{c}{6\eta}\left(1 + \frac{1}{\alpha}\right)\ln\left[\frac{\eta L}{\pi}\sin\left(\frac{\pi\ell}{L}\right)\right] + a_\eta^{(\alpha)}, \tag{98}$$

for $\alpha = 1, 2, \ldots$, c is the central charge, $\eta = 1$ $(\eta = 2)$ for PBC (OBC), and $a_\eta^{(\alpha)}$ is a nonuniversal constant.

The models we are considering have a free-fermion eigenspectra. In this case there exists a standard method [39–41] to calculate the entropies $S_\alpha(L, \ell)$. The method is based on the evaluation of the eigenvalues ν_j $(j = 1, \ldots, \ell)$ of the correlation matrix $\mathbb{C}$, with elements

$$C_{m,n} = \langle\Phi_L|c_m^\dagger c_n|\Phi_R\rangle, \quad m, n = 1, \ldots, \ell. \tag{99}$$

The Rényi entanglement entropies are given by

$$S_\alpha(L, \ell) = \frac{1}{1-\alpha}\sum_{j=1}^{\ell}\ln\left[\nu_j^\alpha + (1-\nu_j)^\alpha\right], \tag{100}$$

and for the case $\alpha = 1$ we have

$$S_1(L, \ell) = -\sum_{j=1}^{\ell}[\nu_j \ln \nu_j + (1-\nu_j)\ln(1-\nu_j)]. \tag{101}$$

For simplicity we are going to present only the cases where the quantum chains are in a periodic lattice. In this case, from Sec. V, the left and right eigenvectors are given by

$$\langle\Phi_L| = \langle 0|\prod_{k\in\{k\}_0}\eta_k, \quad |\Phi_R\rangle = |0\rangle\prod_{k\in\{k\}_0}\eta_k^\dagger, \tag{102}$$

where $\{\eta_k\}$ are the fermionic Fourier modes given in (61). The set $\{k\}_0$ are formed by the quasimomenta in (63) defining the ground state, namely, the ones that give negative values for the quasienergies $\Lambda(k)$, given in (66).

Inserting (63) in (99) we obtain the elements of the correlation matrix

$$C_{m,n} = \frac{1}{4L}\sum_{k\in\{k\}_0} e^{-ik(m-n)}, \tag{103}$$

the sets $\{k\}_0$ depend on the value of N and the lattice size parity. The eigenvalues ν_j $(j = 1, \ldots, \ell)$ of the subsystem correlation matrices with elements $C_{m,n}^{(\ell)}$ $(m, n = 1, \ldots, \ell)$ give the entanglement entropies $S_\alpha(L, \ell)$ in (100) and (101).

In Fig. 8 we show the von Neumann entropy $S_1(L, \ell)$ as a function of $\ln[\frac{L}{\pi}\sin(\frac{\ell\pi}{L})]/3$ for the quantum chain with $N = 3$ and $L = 600$ sites for some values of λ. The results for $S_2(L, \ell)$ and $S_3(L, \ell)$ for the values $\lambda = 1/2$ and $\lambda = 2$ are also shown in Fig. 9. The estimated values of the central charge shown in these figures are obtained from the fit

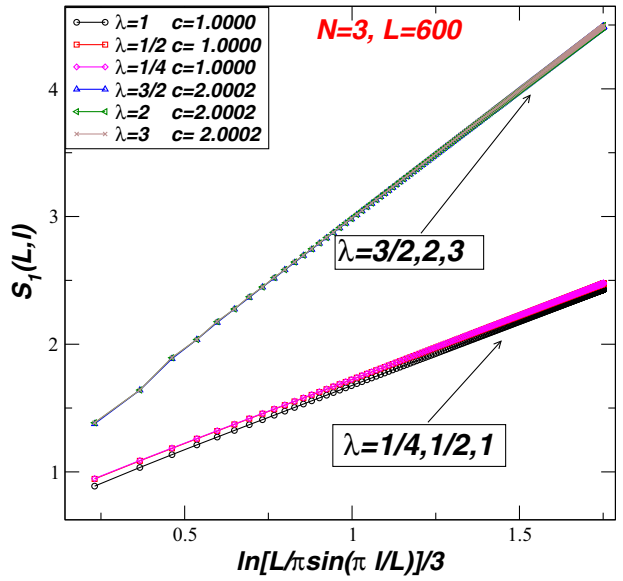

FIG. 8. Von Neumann entanglement entropy $S_1(L, \ell)$, as a function of $\ln[\frac{L}{\pi}\sin(\frac{\ell\pi}{L})]/3$, for some values of λ. The data are for the XX multispin quantum chain with $N = 3$, $L = 600$ sites and PBC.

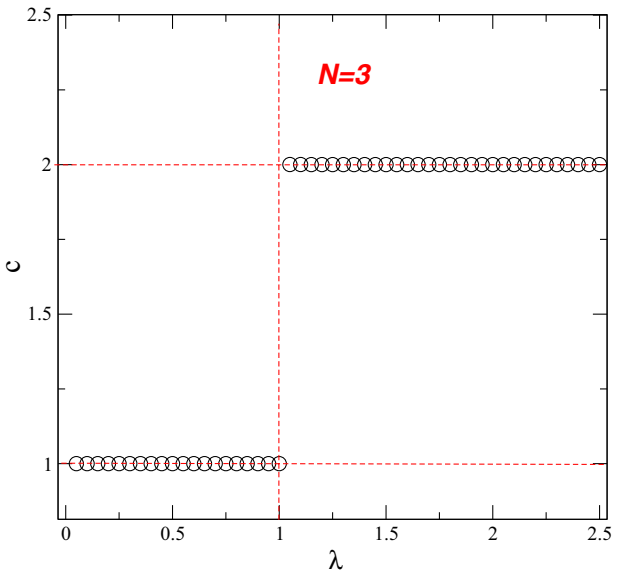

FIG. 10. Estimated values of the central charge c as a function of λ for the multispin XX quantum chain with $N = 3$ and PBC.

$(50 \leqslant \ell \leqslant 300)$ with the expected form (98) quantum chains with $L = 600$ sites. The data in Figs. 8 and 9 show a clear agreement with the prediction (98) with $c = 1$ for $\lambda \leqslant 1$ and $c = 2$ for $\lambda > 1$. This is even clear with the results of Fig. 10 where we show the estimates of the central charge c as a function of λ. The values in this figure are obtained from the fit of $S_1(300, \ell)$ with (98) by considering $50 \leqslant \ell \leqslant 150$. We clearly see a phase transition separating at $\lambda = \lambda_c = 1$ the critical phases with $c = 1$ and $c = 2$, in agreement with the predictions of previous sections. In computing the entropies we should take into account that for $\lambda \leqslant \lambda_c$ we have only two Fermi points, and for $\lambda > \lambda_c$ we have four of them. For general values of $N > 3$ we also found a quite good agreement with the conformal invariance predictions (98).

In Fig. 11 we show our results for the central charge c, as a function of λ for the model with $N = 4$ and $N = 6$. For $N = 4$ (open circles) the phase transition happens at $\lambda = \lambda_c = \frac{1}{3^{1/4}} \approx 0.7598$, separating a phase where $c = 1$ from a phase where $c = N - 1 = 3$. For $N = 6$ (asterisks) the phases are $c = 1$ and $c = N - 1 = 5$, and the transition parameter is $\lambda = \lambda_{c_1} \approx 0.9634$.

In Fig. 12 we show the central charge estimates for $N = 5$ and $N = 7$. We obtain the estimates from the fit of $S_1(900, \ell)$ $(50 < \ell < 450)$ with the expression (98). The model with

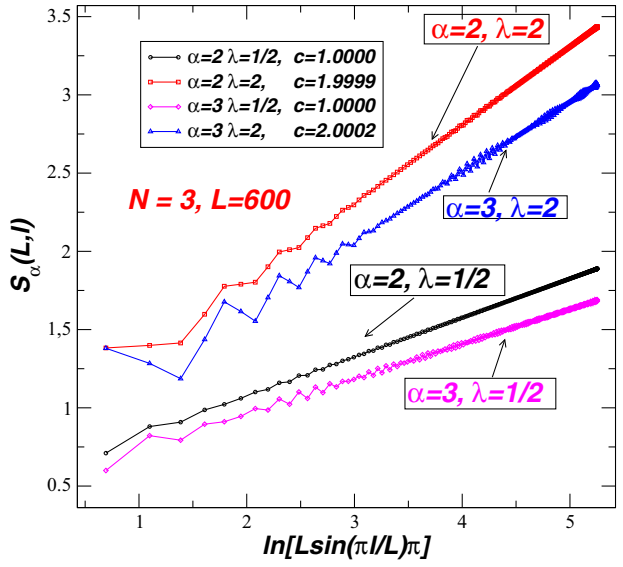

FIG. 9. Rényi entanglement entropies $S_2(L, \ell)$ and $S_3(L, \ell)$, as a function of $\ln[\frac{L}{\pi}\sin(\frac{\ell\pi}{L})]$. The data are for the XX multispin quantum chain with $N = 3$, $L = 600$ sites and PBC.

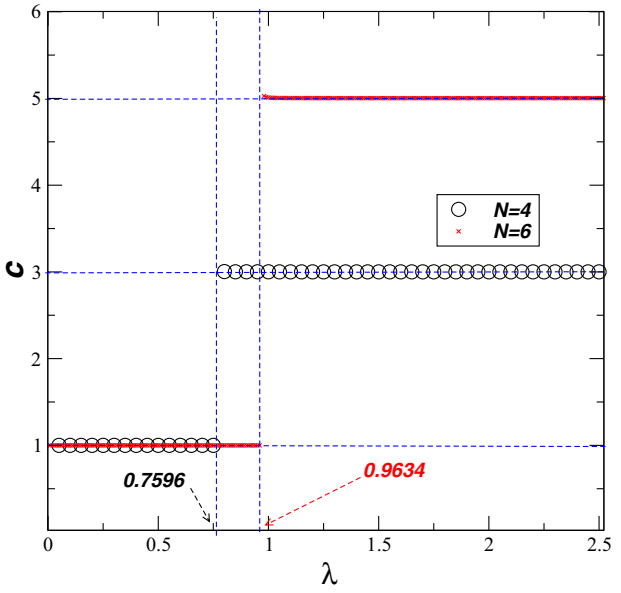

FIG. 11. Estimated values of the central charge c as a function of λ for the multispin XX quantum chains with $N = 3$ and $N = 6$, with PBC.

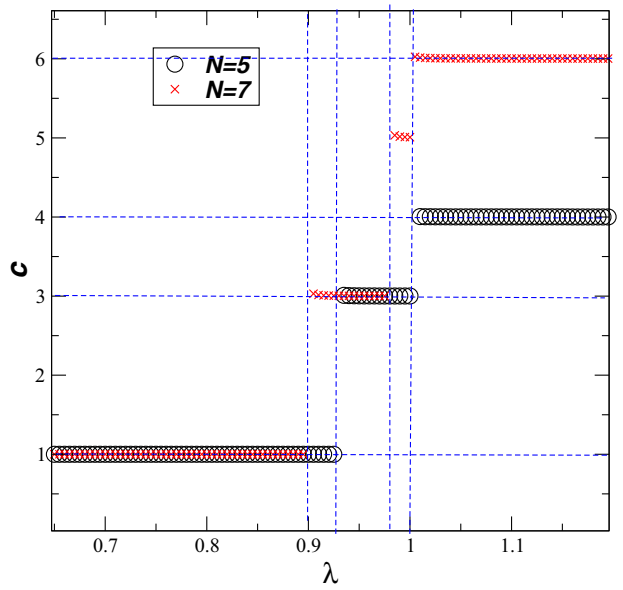

FIG. 12. Estimated values of the central charge c as a function of λ for the multispin XX quantum chains with $N = 5$ and $N = 7$ with PBC.

$N = 5$ (open circles) shows three phases: a phase for $0 < \lambda \leqslant \lambda_{c_1}$ where the model has a central charge $c = 1$, an intermediate phase for $\lambda_{c_1} < \lambda \leqslant \lambda_{c_2}$ where $c = 3$, and a phase, for $\lambda > \lambda_{c_2}$ where $c = N - 1 = 4$. In the case $N = 7$ (open squares) the model has four phases: for $0 < \lambda \leqslant \lambda_{c_1}$ the model has $c = 1$, for $\lambda_{c_1} < \lambda \leqslant \lambda_{c_2}$ the phase has $c = 3$, for $\lambda_{c_2} < \lambda \leqslant \lambda_{c_3}$ the phase has $c = 5$, and for $\lambda > \lambda_{c_4}$ the phase has a central charge $c = N - 1 = 6$. The phase transition points are

$$\lambda_{c_1} = 0.92645, \quad \lambda_{c_2} = 1, \tag{104}$$

for $N = 5$, and for $N = 7$

$$\lambda_{c_1} = 0.89975 \quad \lambda_{c_2} = 0.97899 \quad \lambda_{c_3} = 1. \tag{105}$$

Actually the phase transition points, separating conformal phases with distinct central charges, are precisely the ones where the number of Fermi points N_{FP} changes in the dispersion relation. The central charge is $c = N_{FP}/2$, in agreement with the results of Sec. V.

VII. CONCLUSIONS

In this paper we study the spectral properties of two large families of free-particle quantum chains with multispin interactions. They are considered free because their energies are given by the sum of independent (free) pseudo-energies. In the first family we have parafermionic quantum chains with $Z(N)$ symmetry and $(p + 1)$-multispin interactions ($p = 1, 2, \ldots$). The pseudo-energies forming the eigenenergies of the Hamiltonians satisfy a $Z(N)$ circle exclusion constraint that generalizes the fermion exclusion principle for $Z(2)$. In the second family the models are N-multispin XX models with a $U(1)$ symmetry and described by a free-fermionic eigenspectrum.

The eigenspectra of both models with OBC are described in terms of the same pseudo-energies. These energies are exactly calculated from the roots of special polynomials. In their phase diagram there exists a multicritical point with a dynamical critical exponent $z = (p + 1)/N$. In the particular case where $N = p + 1$ we have $z = 1$, as in conformally invariant quantum chains. Our studies, when both models are in the OBC geometry, indicate that at those multicritical points the quantum chains are conformally invariant. The conformal invariance was tested by exploiting its consequences to the leading finite-size properties of the quantum chains in the finite geometry. These tests were done either analytically or with high numerical precision. The pseudo-energies for the OBC case are obtained from the roots of special polynomials with a known recursion relation. We use a powerful method [20] that allows us to calculate the low-lying energies up to lattice sizes $\sim 10^9$. The numerical tests was done for the $Z(N)$ and XX models with several values of N.

For arbitrary N our results indicate that indeed the models are described at the multicritical points by a conformal field theory. The sound velocity and some of the surface exponents were evaluated exactly.

For the case of a periodic lattice (PBC) the situation is distinct. Due to the non-Hermiticity of the models we have quite distinct physics in the different geometries. For the isotropic models ($\lambda_1 = \lambda_2 = \cdots = \lambda$) the parameter λ is just a harmless overall scaling factor for the models with OBC. However, in the PBC case by changing λ the model, although being critical as in the OBC, undergoes phase transitions.

It is difficult to calculate the eigenspectra of the $Z(N)$ parafermionic quantum chains with PBC. This is not the case for the related N-multispin interacting XX models, since in this case, due to the standard Jordan-Wigner transformation, the Hamiltonian is a sum of bilinear fermion operators. In the case where the chain is translational invariant, as happens for the isotropic model with PBC, the diagonalization follows from a Fourier transform, and all eigenfunctions are given by the composition of Fourier modes. This implies a quite general result: All the translational invariant Hamiltonians (Hermitian or not) that can be expressed after a Jordan-Wigner transformation in a bilinear form will share the same eigenfunctions (not the eigenvalues), and consequently they commute among themselves. The commutation follows directly from the fact that the general Hamiltonian has the form

$$H_L = \sum_{\ell=1}^{L} A_\ell h_\ell, \quad h_\ell = \sum_{i=1}^{L} c_i^\dagger c_{\ell+1}, \tag{106}$$

with $\{A_\ell\} \in \mathbb{C}$, $\ell = 1, \ldots, L$, $c_{i+L} = c_i$, and $[h_\ell, h_m] = 0$.

This means that the study of all the wave functions of a simple model, like the standard two-body XX model, is equivalent to the study of all the eigenfunctions of the general free-fermion quantum chain (106).

The N-multispin XX models with PBC and isotropic coupling λ, considered in this paper, are particular cases of (106). Our results in Secs. V and VI indicate that for the periodic lattices the models undergo phase transitions as we change the value of λ. The finite-size behavior of the eigenspectra, for the models with $N = 3, 4, 5$, and 6, indicates that in general the models are critical and conformally invariant. In each phase the models have distinct central charges, whose values

depend on the value of λ and N. These phases appear because the models, although non-Hermitian, are described by Fermi surfaces and the number of Fermi points N_{FP} depends on the particular value of λ for a given N-multispin XX quantum chain. The central charge has the value $c = N_{FP}/2$. It is important to mention that the energy per site e_∞ of the homogeneous models is the same for the periodic and open boundary cases, only when $N = 2$ where the Hamiltonian is Hermitian. For $N \geqslant 3$ they show distinct values for the different boundary conditions, similarly as happens for the $Z(N)$ free-parafermion Baxter quantum chains, for $N \geqslant 3$ [11].

As a general scenario our results indicate that for small values of $\lambda << 1$ the models are always in a phase with the central charge $c = 1$, and for $\lambda \gg 1$ the models are in a phase with central charge $c = N - 1$. For general values of N the models show intermediate phases with integer values of the central charge ($1 < c < N - 1$), that are formed by independent compositions of $c = 1$ theories, all of them with the lowest conformal dimension $x_p = 1/4$ (see Secs. V and VI).

We conclude by stressing that all these ground states with distinct values of the central charge are also excited states of the general models (106) with $\{A_\ell\}$ arbitrary. An interesting question for the future concerns the phase diagram of the $Z(N)$ N-multispin models with PBC. Are these multiple phases also present?

ACKNOWLEDGMENTS

We thank J. A. Hoyos for discussions. This work was supported in part by the Brazilian agencies FAPESP (Proc.2015/23849-7), CNPq, and CAPES.

[1] T. Schultz, D. Mattis and E. H. Lieb, Two-dimensional Ising model as a soluble problem of many fermions, Rev. Mod. Phys. **36**, 856 (1964).
[2] P. Pfeuty, The one-dimensional Ising model with a transverse field, Ann. Phys. **57**, 79 (1970).
[3] P. Fendley, Free fermions in disguise, J. Phys. A: Math. Theor. **52**, 335002 (2019).
[4] R. J. Baxter, A simple solvable Z_N Hamiltonian, Phys. Lett. A **140**, 155 (1989).
[5] R. J. Baxter, Superintegrable chiral Potts model: Thermodynamic properties, an inverse model and a simple associated Hamiltonian, J. Stat. Phys. **57**, 1 (1989).
[6] P. Fendley, Free parafermions, J. Phys. A: Math. Theor. **47**, 075001 (2014).
[7] R. J. Baxter, The τ_2 model and parafermions, J. Phys. A: Math. Theor. **47**, 315001 (2014).
[8] H. Au-Yang and J. H. H. Perk, Parafermions in the τ_2 model, J. Phys. A: Math. Theor. **47**, 315002 (2014).
[9] H. Au-Yang and J. H. H. Perk, Parafermions in the tau-2 model II, arXiv:1606.06319.
[10] F. C. Alcaraz, M. T. Batchelor, and Z.-Z. Liu, Energy spectrum and critical exponents of the free parafermion Z_N spin chain, J. Phys. A: Math. Theor. **50**, 16LT03 (2017).
[11] F. C. Alcaraz and M. T. Batchelor, Anomalous bulk behavior in the free parafermion *Z(N)* spin chain, Phys. Rev. E **97**, 062118 (2018).
[12] F. C. Alcaraz and R. A. Pimenta, Free fermionic and parafermionic quantum spin chains with multispin interactions, Phys. Rev. B **102**, 121101(R) (2020).
[13] F. C. Alcaraz and R. A. Pimenta, Integrable quantum spin chains with free fermionic and parafermionic spectrum, Phys. Rev. B **102**, 235170 (2020).
[14] S. J. Elman, A. Chapman, and S. T. Flammia, Free Fermions behind the disguise, Commun. Math. Phys. **388**, 969 (2021); A. Chapman, S. T. Flammia, and A. J. Kollár, Free-Fermion subsystem codes, PRX Quantum **3**, 030321 (2022); A. Chapman, S. J. Elman, and R. L. Mann, A unified graph-theoretic framework for Free-Fermion solvability, arXiv:2305.15625.
[15] B. Pozsgay, Quantum circuits with free fermions in disguise, arXiv:2402.02984.
[16] P. Fendley and B. Pozsgay, Free fermions with no Jordan-Wigner transformation, arXiv:2310.19897.
[17] P. D. Mannheim, PT symmetry as a necessary and sufficient condition for unitary time evolution, Phil. Tram. R. Soc. A **371**, 2120060 (2012).
[18] F. C. Alcaraz and R. A. Pimenta, Free-parafermionic $Z(N)$ and free-fermionic XY quantum chains, Phys. Rev. E **104**, 054121 (2021).
[19] F. C. Alcaraz, R. A. Pimenta and J. Sirker, Ising analogs of quantum spin chains with multispin interactions, Phys. Rev. B **107**, 235136 (2023).
[20] F. C. Alcaraz, J. A. Hoyos, and R. A. Pimenta, Powerful method to evaluate the gaps of free-particle quantum critical chains, Phys. Rev. B **104**, 174206 (2021).
[21] R. A. Henry and M. T. Batchelor, Exceptional points in the Baxter-Fendley free parafermion model, Sci. Post **15**, 016 (2023).
[22] F. C. Alcaraz, M. N. Barber, and M. T. Batchelor, Conformal invariance, the XXZ chain and the operator content of two-dimensional critical systems, Ann. Phys. **182**, 280 (1988).
[23] J. L. Cardy, Operator content of two-dimensional conformally invariant theories, Nucl. Phys. B **270**, 186 (1986).
[24] Q. I. Rahman and G. Schmeisser, in *Analytic Theory of Polynomials*, edited by H. G. Dales and P. M. Neumanni, London Mathematical Society Monographs Vol. 26 (Clarendon Press, Oxford, 2002; Academic Press, New York, 1983).
[25] F. C. Alcaraz, J. A. Hoyos and R. A. Pimenta, Random free-fermion quantum spin chain with multispin interactions, Phys. Rev. B **108**, 214413 (2023).
[26] H. W. J. Blöte, J. L. Cardy and M. P. Nightingale, Conformal invariance, the central charge, and universal finite-size amplitudes at criticality, Phys. Rev. Lett. **56**, 742 (1986).
[27] L. Titvinidze and G. Japaridze, Phase diagram of the spin extended model, Eur. Phys. J. B **32**, 383 (2003).
[28] I. Affleck, Universal term in the free energy at a critical point and conformal anomaly, Phys. Rev. Lett. **56**, 746 (1986).
[29] L. P. Kadanoff, Multicritical behavior at the Kosterlitz-Thouless critical point, Ann. Phys. **120**, 39 (1979).
[30] L. P. Kadanoff and A. Brown, Correlation functions on the critical lines of the Baxter and Ashkin-Teller models, Ann. Phys. **121**, 318 (1979).
[31] F. C. Alcaraz, M. Baake and V. Rittenberg, Operator content of the XXZ chain, J. Phys. A: Math. Gen. **21**, L117 (1988).

[32] F. C. Alcaraz, U. Grimm and V. Rittenberg, The XXZ Heisenberg chain, conformal invariance and the operator content of $c < 1$ systems, Nucl. Phys. B **316**, 735 (1989).
[33] V. Alba, M. Fagotti, and P. Calabrese, Entanglement entropy of excited states, J. Stat. Mech. (2009) P10020.
[34] Y.-B. Guo, Y.-C. Yu, R.-Z. Huang, L.-P. Yang, R.-Z. Chi, H.-J. Liao, and T. Xiang, Entanglement entropy of non-Hermitian free fermions, J. Phys.: Condens. Matter **33**, 475502 (2021).
[35] C. Holzhey, F. Larsen, and F. Wilczek, Geometric and renormalized entropy in conformal field theory, Nucl. Phys. B **424**, 443 (1994).
[36] P. Calabrese and J. L. Cardy, Entanglement entropy and quantum field theory, J. Stat. Mech. (2004) P06002.
[37] P. Calabrese and J. L. Cardy, Entanglement entropy and conformal field theory, J. Phys. A: Math. Theor. **42**, 504005 (2009).
[38] V. Korepin, Universality of entropy scaling in one dimensional gapless models, Phys. Rev. Lett. **92**, 096402 (2004).
[39] G. Vidal, J. I. Latorre, E. Rico and A. Kitaev, Entanglement in quantum critical phenomena, Phys. Rev. Lett. **90**, 227902 (2003).
[40] I. Peschel, Calculation of reduced density matrices from correlation functions, J. Phys. A: Math. Gen. **36**, L205 (2003).
[41] P.-Y. Chang, J-S. You, X. Wen, and S. Ryu, Entanglement spectrum and entropy in topological non-Hermitian systems and nonunitary conformal field theory, Phys. Rev. Res. **2**, 033069 (2020).